Perceptual and memory neural processes underlie short and long-term non-reinforced behavioral change

Rotem Botvinik-Nezer[1,2], Tom Salomon[2] and Tom Schonberg[1,2*]

[1] Sagol School of Neuroscience, Tel Aviv University, Tel Aviv, Israel.

[2] Faculty of Life Sciences, Department of Neurobiology, Tel Aviv University, Tel Aviv, Israel.

* Corresponding author.

Studies and behavioral interventions have focused on reinforcement and context change as means to influence preferences. Cue-approach training (CAT) has been shown to induce preference changes lasting months, towards items that were merely paired with a neutral cue and a speeded response without reinforcement. We scanned 36 participants with fMRI during a passive viewing task before, after and one month following CAT to study the neural basis of the representation and modification of preferences without reinforcements. We found that enhanced visual processing in the short-term, memory processes in the long-term and less involvement of top-down processes, underlie value change. These results show for the first time a change in the neural representation of items in perceptual regions immediately after training, putatively influencing long-term memory accessibility. Our findings set the ground for new theories and clinical interventions manifesting automatic bottom-up instead of top-down processes to accomplish long-term behavioral change.

Introduction

When faced with a choice between two food items, how do people make a choice? How can choices be affected to promote well-being? Understanding how

preferences are constructed and modified is a major challenge in the research of human behavior with broad implications, from basic science to interventions for long-lasting behavioral change (Marteau, Hollands, & Fletcher, 2012; Vlaev, Chater, Stewart, & Brown, 2011).

The basic question of how preferences are represented in the brain has been the center of many animal and human studies alike (Kable & Glimcher, 2009; Padoa-Schioppa, 2011; Padoa-Schioppa & Cai, 2011; Rangel, Camerer, & Montague, 2008). These studies are usually conducted under the assumption that decisions are made based on the comparison of subjective values of each choice alternative (Padoa-Schioppa, 2011; Rangel et al., 2008; Vlaev et al., 2011). Previous studies identified a network of brain regions involved in value-based decision-making, mainly the ventromedial prefrontal cortex (vmPFC) and orbitofrontal cortex (OFC), which are considered the regions where values are computed and represented (D. J. Levy & Glimcher, 2012; Padoa-Schioppa, 2011; Padoa-Schioppa & Cai, 2011). The striatum has been implicated in reinforcement learning (Balleine, 2005), habit formation (Yin & Knowlton, 2006) and decision-to-motor transform together with the lateral prefrontal cortex (Cai, Kim, & Lee, 2011; Cai & Padoa-Schioppa, 2014).

The field of decision-making has focused mainly on two types of choice behaviors: Goal-directed (model-based) and habit-based (model-free) (Balleine & O'Doherty, 2010). In goal-directed behavior, the value of each available option is computed and the behavior is guided by the potential value of the outcomes. In contrast, habit-based behavior occurs when an action is repeated and reinforced multiple times, omitting the dependency on the potential value of the outcome. These two types of behavior involve reinforcement, either during the evaluation (or learning) of a potential outcome or during the formation of a habit (Rangel et al., 2008). However, in a novel and unique

paradigm for behavioral change, named cue-approach training (CAT), preferences were successfully modified in the absence of external reinforcement (Schonberg et al., 2014).

In the CAT paradigm, the mere association of images of items with a cue and a speeded button-press response leads to preference changes lasting months following a single training session (Salomon et al., 2018; Schonberg et al., 2014). This paradigm putatively affects choices through automatic processes without external reinforcement (Marteau et al., 2012) and thus allows to obtain novel knowledge on how preferences are represented and affected without external reinforcement or context change. Experiments with CAT commonly consist of three main phases: An evaluation phase to obtain initial subjective preferences for various items, a training phase and a probe phase to evaluate preferences modification with binary choices. During CAT, images of items (originally snack-food items) appear on the screen one by one, and participants are instructed to press a button as fast as they can in response to a delayed cue. Unbeknownst to the participants, some of the items are consistently paired with the cue and response (these are termed ‘Go items’) while the rest of the items are not (‘NoGo items’). In a subsequent probe phase, participants choose their preferred item for consumption between pairs of items with similar initial subjective values, in which only one was a Go item, previously paired with the cued button press. Replicated results from multiple samples (Bakkour, Lewis-Peacock, Poldrack, & Schonberg, 2016; Salomon et al., 2018; Schonberg et al., 2014; Veling et al., 2017; Zoltak, Veling, Chen, & Holland, 2017) show that participants significantly choose high-value Go over high-value NoGo items.

Recently, Salomon et al. (2018) demonstrated that CAT can be used to change preferences towards various types of stimuli (i.e. unfamiliar faces, fractal art images

and positive affective images) with different types of cues (i.e. neutral auditory, aversive auditory and visual cues), showing that the underlying mechanism of the task is general. Furthermore, preferences' change has been shown to last up to six months following a single training session lasting less than one hour, thus endorsing the applicability of CAT as a real-world intervention.

CAT is performed on single items and thus changes preferences of individual items, later manifested in binary choice. Furthermore, its low-level nature, not involving external reinforcement or high-level executive control, provides a unique opportunity to study preference representation and modification in the brain.

Previous studies with CAT were able to predominantly shed light on the neural signature of preference change during choice. Eye-gaze data revealed that during choices, attention is drawn towards Go items more compared to NoGo items even when the Go items were not chosen (Schonberg et al., 2014). Functional MRI results demonstrated an enhanced BOLD signal in the vmPFC during choices of high-value Go items alone and compared to NoGo items (Schonberg et al., 2014). These results indicate enhanced value processing during choices of Go compared to choices of NoGo items, but do not reveal the mechanism of value change in the single item level. A multi-voxel pattern analysis study was also not able to point to differences induced during CAT between Go and NoGo items in perceptual, memory or valuation components (Bakkour, Lewis-Peacock, et al., 2016). Putatively, functional imaging during training was uninformative as to the source of the value changes occurring during training due to widespread co-activation of the motor and sensory systems during Go items presentations, masking potential differences of Go versus NoGo items. Moreover, no attempt has been made yet to investigate the neural mechanism of the long-term effect of CAT.

Therefore, here we introduce a novel phase to shed light on how preferences toward individual items are represented and modified in the brain. We added a passive viewing task whereby items were presented individually on the screen before and after CAT. During this task, items were individually presented on the screen without any manipulation, while participants performed a sham counting task (Fig. 1b,d). We tested the different neural responses to Go versus NoGo items after training compared to baseline, as well as one month following training compared to baseline. Regions in the brain showing plasticity after training and one month later shed light on the general mechanisms of preference representation in the brain and specifically on how non-externally reinforced training leads to robust long-lasting preference changes.

Overall, current evidence suggests that the immediate behavioral change following CAT might involve attention modification and value enhancement (Schonberg et al., 2014; Veling et al., 2017). Furthermore, the long-lasting nature of the effect raises the possibility that memory processes are also involved. Therefore, we hypothesized that preferences are highly dependent on attentional and memory-related mechanisms, affecting value representation. In our pre-registered hypotheses (https://osf.io/q8yct/?view_only=360ad8ba027b4a85ab56b1586d6ad6c9), we predicted greater BOLD activity after CAT in response to high-value Go items in episodic memory-related regions in the medio-temporal lobe, top-down attention-related dorsal parietal cortex and prefrontal value-related regions. In addition, we hypothesized we will replicate previous CAT results showing a significant behavioral effect of choosing high-value Go over high-value NoGo items during probe and increased BOLD activity in the vmPFC during choices of high-value Go items (Bakkour, Leuker, et al., 2016; Bakkour, Lewis-Peacock, et al., 2016; Salomon et al., 2018; Schonberg et al., 2014; Veling et al., 2017; Zoltak et al., 2017).

Most current behavioral interventions for treating conditions such as addictions and eating-disorders rely on effortful control and on reinforcement. However, previous studies showed that these interventions tend to fail in the long term (Christiansen, Bruun, Madsen, & Richelsen, 2007; Jeffery et al., 2000; Prochaska, Delucchi, & Hall, 2004). Results from this study will shed light on the representation and modification of preferences and lead to new and better interventions for long-term behavioral change.

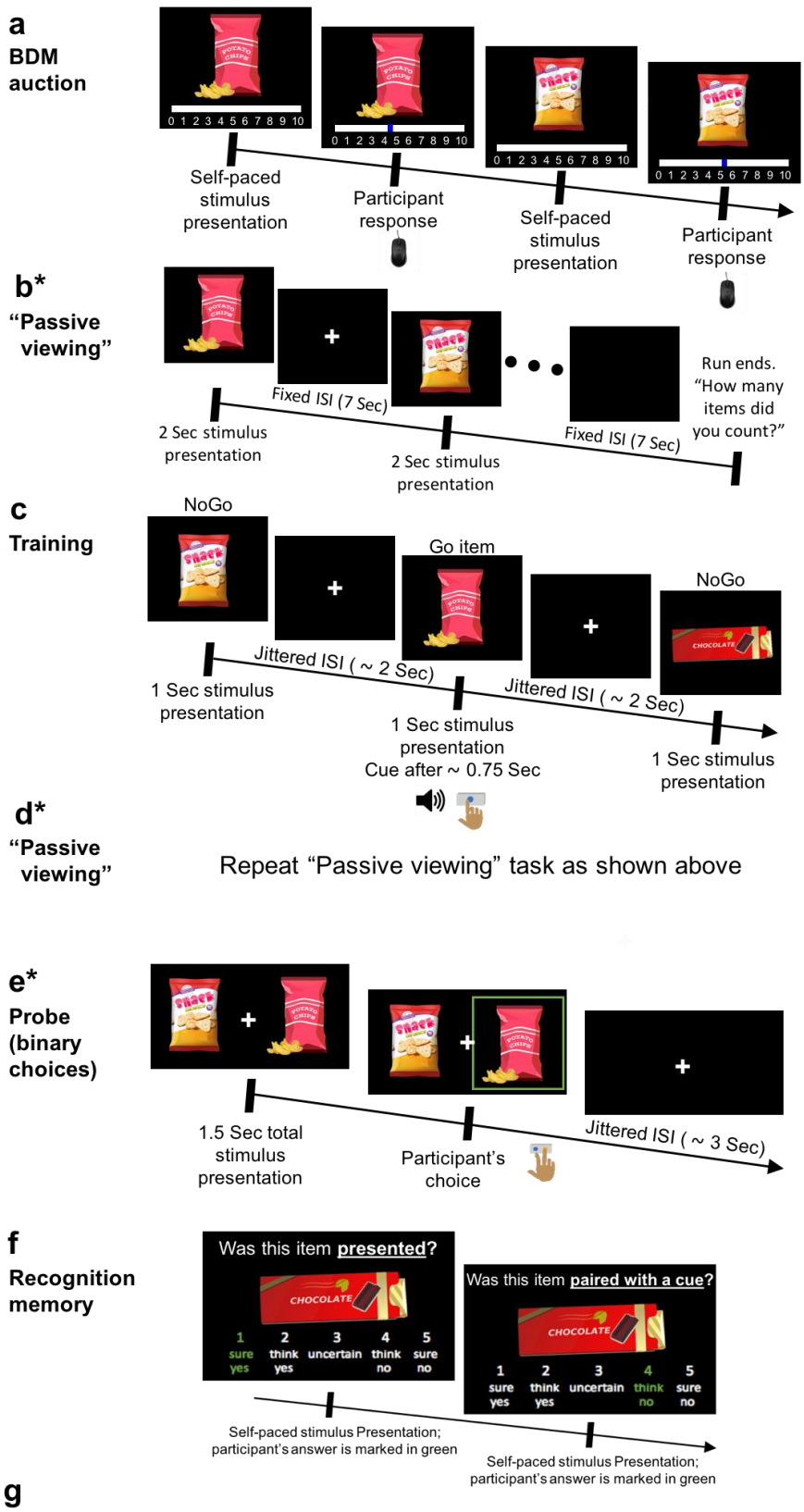
a
BDM auction
0 1 2 3 4 5 6 7 8 9 10
Self-paced stimulus presentation
Participant response
Self-paced stimulus presentation
Participant response
b*
"Passive viewing"
Fixed ISI (7 Sec)
2 Sec stimulus presentation
2 Sec stimulus presentation
Fixed ISI (7 Sec)
Run ends. "How many items did you count?"
c
Training
NoGo
Go item
NoGo
Jittered ISI (~ 2 Sec)
Jittered ISI (~ 2 Sec)
1 Sec stimulus presentation
1 Sec stimulus presentation
Cue after ~ 0.75 Sec
1 Sec stimulus presentation
d*
"Passive viewing"
Repeat "Passive viewing" task as shown above
e*
Probe (binary choices)
1.5 Sec total stimulus presentation
Participant's choice
Jittered ISI (~ 3 Sec)
f
Recognition memory
Was this item presented?
1 sure yes
2 think yes
3 uncertain
4 think no
5 sure no
Was this item paired with a cue?
1 sure yes
2 think yes
3 uncertain
4 think no
5 sure no
Self-paced stimulus Presentation; participant's answer is marked in green
Self-paced stimulus Presentation; participant's answer is marked in green
g
BDM auction
Repeat BDM auction as shown above

Figure 1. *Outline of the experimental procedures. Procedures performed inside the MRI scanner (during a functional scan) are marked with an asterisk. (a) Initial preferences were evaluated using the Becker–DeGroot–Marschak (BDM) auction procedure* (Becker, DeGroot, & Marschak, 1964)*. (b) "Passive viewing", a new task in which items are individually presented on the screen, while participants passively observe them and perform a sham counting task. (c) Cue-approach training: Participants were instructed to press a button as fast as they could whenever they heard an auditory cue, and before the item disappeared from the screen. Items were presented on the screen one by one. Go items were consistently paired with the cue and button press response, while NoGo items were not. (d) The "passive viewing" task was repeated after training. (e) In the probe task, participants chose their preferred item between pairs of items with similar initial subjective preferences, one Go and one NoGo item. (f) A recognition memory task. (g) The BDM auction was repeated. . Stages e-g were performed again in the one-month follow-up session.*

Results

Behavioral probe results

After CAT. Participants (N = 36) significantly preferred Go over NoGo items in high-value probe choices (mean = 0.590, SE = 0.032, Z = 2.823 *P* = 0.002, one-sided logistic regression) and marginally also in low-value probe choices (mean = 0.561, SE = 0.038, Z = 1.639 *P* = 0.051; Fig. 2). The proportion of Go items choices was significantly higher for high-value compared to low-value items (indicating a differential effect of CAT on preference for stimuli of the two value categories, Z = 2.184, *P* = 0.015, one-sided logistic regression). These results were predicted based on previous studies and replicated them (Bakkour, Leuker et al., 2016; Salomon et al., 2018; Schonberg et al., 2014).

One-month follow-up. One month following training (mean = 30.26 days, SD = 9.93 days, N = 27) participants significantly chose Go over NoGo items in both high-value (mean = 0.563, SE = 0.035, Z = 1.854, *P* = 0.032) and low-value (mean = 0.572, SE = 0.039, Z = 1.948, *P* = 0.026) probe trials. There was no differential effect in this session (Z = 0.622, *P* = 0.267).

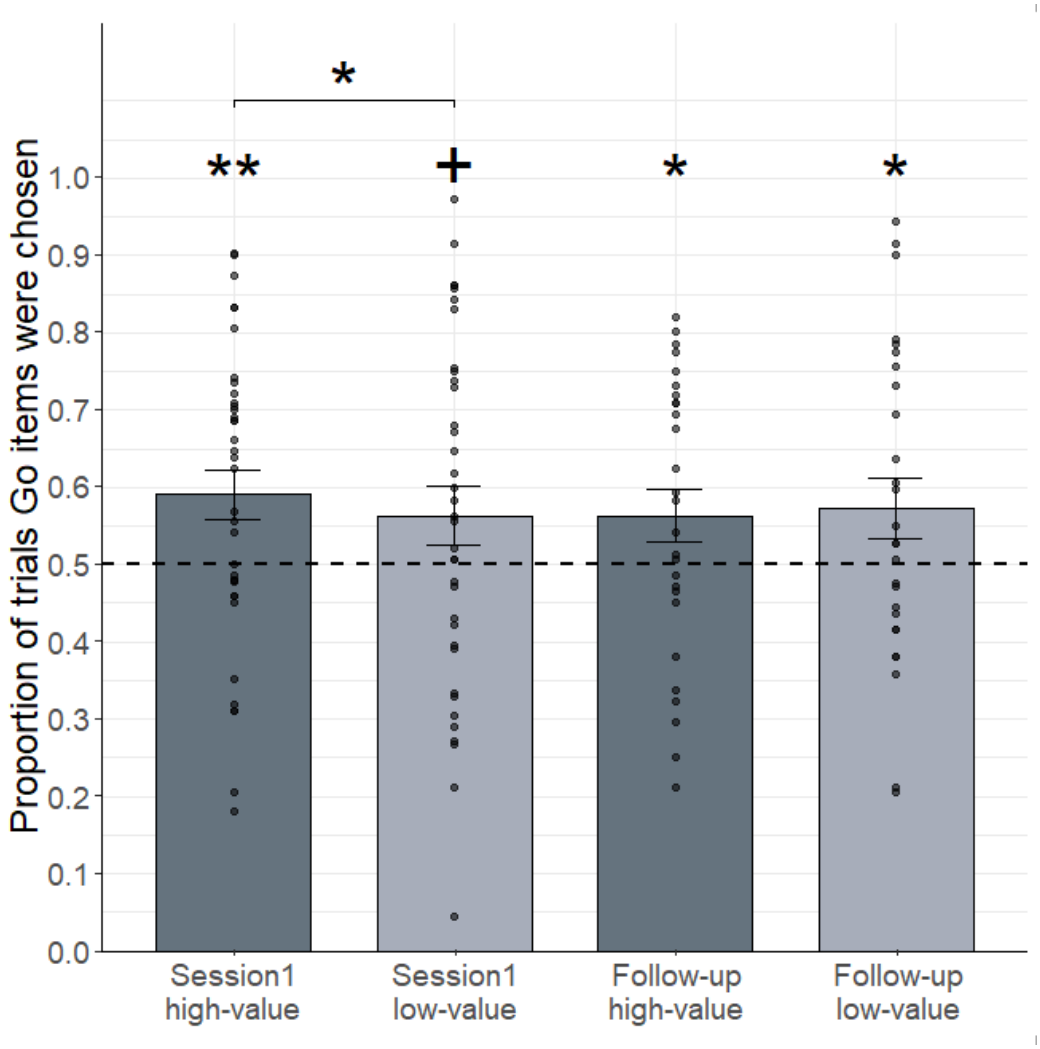

***Figure 2**. Behavioral results of Go choices during probe. Mean proportion of trials in which participants chose Go over NoGo items are presented for high-value (dark gray) and low-value (light gray) probe pairs, for each session (session1 / follow-up). Means of the single participants are shown with dots over each bar. The dashed line indicates chance level of 50%, error bars represent standard error of the mean. Asterisks reflect statistical significance in a one-tailed logistic regression analysis. Asterisks above each line represent proportions higher than chance (log-odds = 0, odds-ratio = 1). Asterisks above pairs of bars represent differential effect between the two value categories; +P < 0.1, *P < 0.05, **P < 0.005.*

Imaging results

Behavioral results with snack food items from previous studies (Bakkour, Lewis-Peacock, et al., 2016; Salomon et al., 2018; Schonberg et al., 2014) and from the current study demonstrated a consistent differential pattern of the change of

preferences across value level: Preferences modifications were more robust for high-value compared to low-value items. Therefore, in our imaging results, we chose to focus on the functional changes in the representation of high-value items, which had more dominant behavioral modification effect. We further tested two kinds of relations between the behavioral effect and the neural response: *Modulation across items*, meaning that the change in activity was stronger for items that were later more preferred during the subsequent probe phase (within-participant first-level parametric modulation); and *correlation across participants*, meaning that the change in activity was stronger for participants that later showed a stronger behavioral effect, quantified as higher ratio of choosing high-value Go over high-value NoGo items (between-participants group-level correlation). Finally, for a subset of three pre-hypothesized and pre-registered regions (vmPFC, hippocampus and superior parietal lobule) we performed a small volume correction (SVC) analysis (see online methods).

Untresholded images of all contrasts presented here can be found on NeuroVault (K. J. Gorgolewski et al., 2015) (https://neurovault.org/collections/TTZTGQNU/)

Passive viewing imaging results

To investigate the functional changes in the response to the individual items following CAT, we scanned participants with fMRI while they were passively viewing the items. Participants completed this task before, after and one month following CAT (N = 36; follow-up N = 27).

After CAT *(Fig. 3, for description of all activations see Supplementary Table 2).* BOLD activity while passively viewing high-value Go compared to passively viewing high-value NoGo items was increased after compared to before CAT in the left and right

occipital and temporal lobes (Fig. 3a), along the ventral visual processing pathway (Goodale & Milner, 1992).

Results of the SVC analyses revealed enhanced BOLD activity during passive viewing of high-value Go items after compared to before CAT in the vmPFC (Fig. 3b).

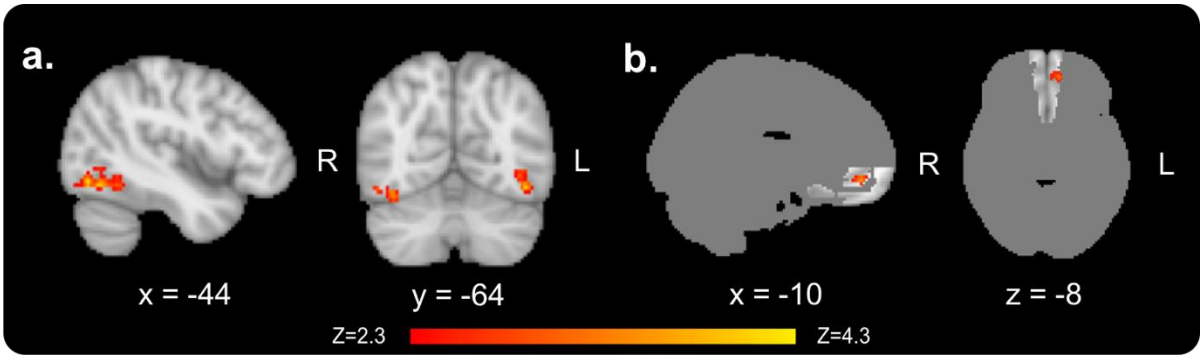

Figure 3. *fMRI results from the passive viewing task after compared to before CAT. (a) Enhanced BOLD activity in bilateral occipito-temporal regions, for high-value Go compared to high-value NoGo items (whole-brain analysis). (b) Enhanced BOLD activity in the vmPFC in response to high-value Go items (Small volume corrected results; the mask used is presented on a dark grey brain silhouette). For description of all activations see Supplementary Table 2.*

One-month follow-up *(Fig. 4, for description of all activations see Supplementary Table 3).* Comparison of the BOLD activity in response to high-value Go items in the follow-up compared to before CAT did not reveal significant clusters with whole-brain correction. However, similar to the short-term change, BOLD activity in the vmPFC was found to be enhanced with SVC analyses (Fig. 4a). In addition, BOLD activity in the left orbitofrontal cortex (OFC) in response to high-value Go items was positively modulated by the choice effect across items in the follow-up compared to before CAT (whole-brain analysis; Fig. 4b). SVC analyses revealed that BOLD activity in response to high-value Go items in the right anterior hippocampus was positively modulated by the choice effect across items in the follow-up compared to before training (Fig. 4c), while BOLD activity in response to high-value Go minus high-value NoGo items in the

right SPL was negatively correlated with the choice effect across participants in the follow-up compared to before training (Fig. 4d).

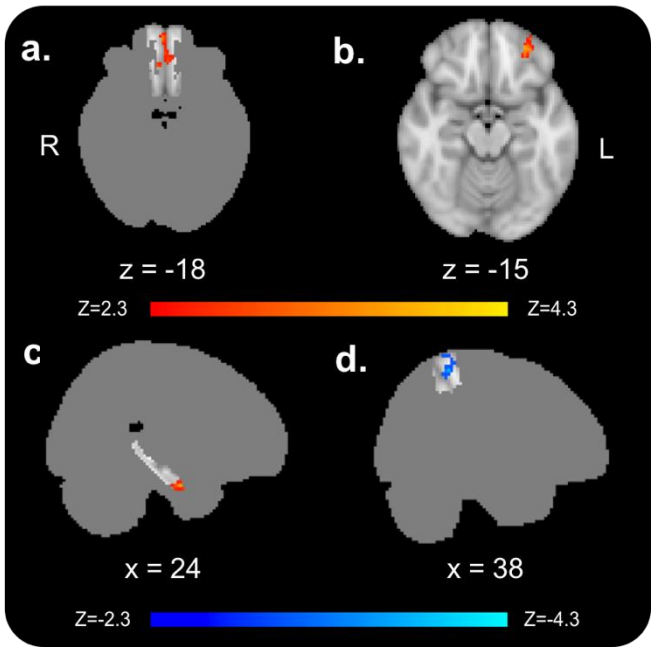

Figure 4. *fMRI results from the passive viewing task in the one-month follow-up compared to before CAT. (a) Enhanced BOLD activity in response to high-value Go items in the vmPFC (small volume corrected). (b) BOLD activity in response to high-value Go items in the left OFC was positively modulated by the choice effect across items (whole-brain analysis). (c) BOLD activity in response to high-value Go items in the right anterior hippocampus was positively modulated by the choice effect across items (small volume corrected). (d) BOLD activity in response to high-value Go minus high-value NoGo items in the right SPL was negatively correlated with the choice effect across participants (small volume corrected). The masks used for the small volume correction (SVC) analyses are presented on a dark grey brain silhouette. For description of all activations see Supplementary Table 3.*

Inspection of the uncorrected results ($z > 2.3$) revealed increased visual enhancement for high-value Go compared to high-value NoGo items in the follow-up compared to before CAT, in visual regions similar to the ones found to be enhanced after CAT. However, these clusters did not exceed statistical significance following whole-brain cluster correction and were not pre-registered; therefore, we did not perform an SVC analysis for these regions.

Probe imaging results

To investigate the functional response during choices, we scanned participants with fMRI while they completed the probe (binary choices) phase, as was done in previous studies (Bakkour, Lewis-Peacock, et al., 2016; Schonberg et al., 2014). Participants completed the probe task after CAT (N = 33) as well as in the one-month follow-up for the first time (N = 25).

After CAT *(Fig. 5, for description of all activations see Supplementary Table 4).* BOLD activity was stronger during choices of high-value Go over high-value NoGo items compared to choices of high-value NoGo over high-value Go items in bilateral visual regions and bilateral central opercular cortex and Heschl's gyrus (Fig. 5a). In addition, BOLD activity in the striatum while choosing high-value Go compared to choosing high-value NoGo items after CAT was negatively correlated with the choice effect across participants (the ratio of choosing high-value Go items during probe; Fig. 5b) and negatively modulated by the choice affect across items (Fig. 5c). SVC analysis revealed that BOLD activity in the right SPL while choosing high-value Go items after CAT was negatively correlated with the choice effect across participants (Fig. 5d) and negatively modulated by the choice effect across items (Fig. 5e).

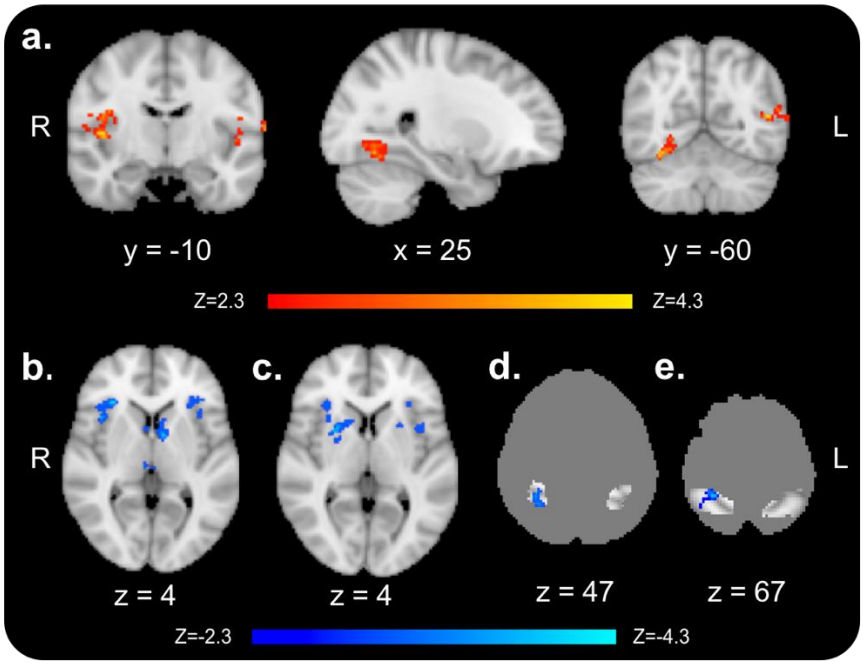

Figure 5. *fMRI results from the probe task after CAT: (a) Enhanced BOLD activity during choices of high-value Go compared to choices of high-value NoGo items in bilateral visual regions and bilateral central opercular cortex and Heschl's gyrus (whole-brain analysis). (b) BOLD response negatively correlated with the choice effect across participants and (c) negatively modulated by the choice effect across items, during choices of high-value Go over high-value NoGo items in the striatum as well as other regions (whole-brain analysis). (d) BOLD response negatively correlated with the choice effect across participants and (e) negatively modulated by the choice effect across items, during choices of high-value Go compared to high-value NoGo items, in the right SPL (small volume corrected). The masks used are presented on a dark grey brain silhouette. For description of all activations see Supplementary Table 4.*

One-month follow-up *(Fig. 6, for description of all activations see Supplementary Table 5).* BOLD activity in the precuneus, bilateral superior occipital cortex and bilateral middle and superior temporal gyrus while choosing high-value Go items in the follow-up was positively modulated by the choice effect across items (Fig. 6a). BOLD activity in the precuneus/posterior cingulate cortex (PCC) and right post-central gyrus while choosing high-value Go items in the follow-up was positively correlated with the choice effect across participants (Fig. 6b).

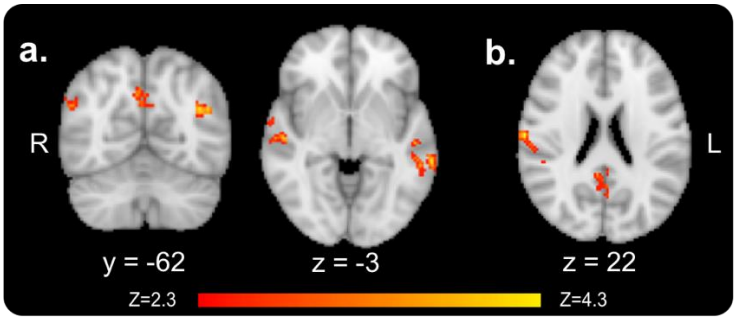

Figure 6. *fMRI results from the probe task in the one-month follow-up: BOLD activity during choices of high-value Go items (whole-brain analyses) was (a) positively modulated by the choice effect across items in the precuneus, bilateral superior occipital cortex and bilateral middle and superior temporal gyrus and (b) positively correlated with the choice effect across participants in the precuneus/posterior cingulate cortex (PCC) and right post-central gyrus. For description of all activations see Supplementary Table 5.*

Discussion

Research of value-based decision-making and behavioral change mainly focused on reinforcement and context change as means to change preferences (Martino, Kumaran, Seymour, & Dolan, 2006; Rangel et al., 2008; Tversky & Kahneman, 1986). The cue-approach training (CAT) paradigm has been shown to change preferences using the mere association of a cue and a speeded button response without external reinforcement. The paradigm is highly replicable with dozens of studies demonstrating the ability to change behavior for months with various stimuli and cues (Bakkour, Leuker, et al., 2016; Bakkour, Lewis-Peacock, et al., 2016; Salomon et al., 2018; Schonberg et al., 2014; Veling et al., 2017; Zoltak et al., 2017). The behavioral results obtained in the current study replicated previous studies, demonstrating enhanced preferences towards high-valued cued (high-value Go) compared to high-valued non-cued (high-value NoGo) items following CAT (Bakkour, Leuker, et al., 2016; Bakkour, Lewis-Peacock, et al., 2016; Salomon et al., 2018; Schonberg et al., 2014; Veling et al., 2017; Zoltak et al., 2017). Importantly, CAT

utilizes low-level associations to induce long-term change of preferences at the item level, without external reinforcement or high-level self-control mechanisms, and thus it provides a unique opportunity to study how preferences are represented and modified in the brain at the individual item level in the absence of reinforcement. Here we introduced a new passive viewing task to study the functional plasticity of the response to single items before, after and one month following CAT, in order to deepen our understanding of the neural mechanisms involved in non-reinforced preferences modification, both in the short and in the long term. Prior to data analysis, we predicted and pre-registered that the underlying neural mechanisms will involve memory, attention and value-related brain regions.

Functional changes in the short and long-term

Passive viewing

We found enhancement of visual processing for Go compared to NoGo items after training during passive viewing. We show for the first time that activity in high-level visual processing occipito-temporal cortex is related to subjective values without rewards. By recording eye-gaze from a sub-group of our participants during this task, we found that enhanced activity in occipito-temporal visual cortex was probably not the result of longer gaze duration on paired items (see Supplementary Data). Activity in low and high-level visual regions was previously shown to be related to value, but this activity was related to past rewards and not to subjective values (Serences, 2008). We also found evidence for enhanced BOLD response in the vmPFC for cued items, after CAT and in the one-month follow-up, indicating a long-lasting value change signature (Lebreton, Jorge, Michel, Thirion, & Pessiglione, 2009; I. Levy, Lazzaro, Rutledge, & Glimcher, 2011) of individual items not during choices. These results

reveal for the first time an item-level value change during passive viewing (I. Levy et al., 2011; Serences, 2008), in accordance with previous findings of enhanced activity in the vmPFC during binary choices of more preferred high-value Go items (Bakkour, Lewis-Peacock, et al., 2016; Schonberg et al., 2014). In addition, this is the first time, to the best of our knowledge, that such enhancement in value-related prefrontal regions is found one month following a behavioral change paradigm.

In the follow-up session, we further found that the long-term behavioral change was related to plasticity in memory, attention and value-related brain regions. In addition to the enhancement of activity in the vmPFC described above, the change in BOLD response to the cued Go items in the left OFC and right hippocampus was positively modulated by the choice effect across items, meaning that activity in these regions was stronger while viewing Go items which were later chosen more during the subsequent probe phase.

We suggest that the functional changes in the bilateral occipito-temporal visual regions reflect modifications in the representation of the paired items (Grill-Spector, 2003; Grill-Spector, Kourtzi, & Kanwisher, 2001; Ishai, Ungerleider, Martin, & Haxby, 2000), following the low-level association of visual images with auditory cues and motor responses during training. The bottom-up enhanced perceptual processing and representation of paired items led to enhanced value-related processing, reflected as enhanced activity in the vmPFC, and thus to choices of these items over non-paired items (Serences, 2008). The bottom-up enhanced short-term perceptual processing enhancement further affected the encoding and accessibility of paired items and their related associations in memory for the long-term. This suggests why in the one-month follow-up, visual processing was enhanced to a lesser extent, while memory-related processes drove the long-term behavioral effect.

In addition to these results, the change in BOLD response in the long-term (follow-up greater than before CAT) in the right SPL was negatively correlated with the choice effect across participants; i.e. participants with overall greater behavioral change demonstrated reduced change of BOLD response to high-value Go items in this region. This finding suggest reduced involvement of top-down attention mechanisms during passive viewing of Go compared to NoGo items (Culham & Kanwisher, 2001), importantly suggesting that the behavioral change following CAT is a result of an influence on automatic processes..

Binary choices

We further compared BOLD response during choices of paired versus non-paired items during the probe phase. BOLD response was enhanced mainly in visual and auditory related regions in the occipital and temporal lobes. These findings suggest that in the short-term, retrieval of the low-level visual and auditory associations, which were constructed during training, resulted in Go items' choices. In addition, these findings strengthen the finding of enhanced perceptual processing of Go items during passive viewing by indicating that visual, as well as auditory processing, are also enhanced during choices of Go over NoGo items, suggesting that enhanced bottom-up processing is putatively driving the short-term enhanced preferences towards Go items.

Activity in the right SPL during choices of paired items was negatively modulated by the choice effect across items as well as negatively correlated with the choice effect across participants (though in a more posterior and inferior region), indicating that top-down attentional mechanisms were less involved during choices of Go compared to choices of NoGo items (Culham & Kanwisher, 2001). These results provide further

neural evidence of the automatic nature of the mechanism underlying the behavioral change following CAT.

Activity in the striatum, a region known to be involved in reinforcement learning and habit-based learning (Daniel & Pollmann, 2014; Yin & Knowlton, 2006), was also negatively correlated with choices of paired over non-paired items, both in a parametric modulation across items (mainly in the right putamen) as well as a correlation with the behavioral effect across participants (mainly in the left caudate). These findings potentially suggest that cue-approach training shifted the process of goal-directed decision-making during binary choices to be more automatic and based on non-reinforced mechanisms. Although previous studies included fMRI during the probe phase, this is the first study with CAT to observe these effects and thus it remains to be replicated in future studies (Bakkour, Lewis-Peacock, et al., 2016; Schonberg et al., 2014).

In the follow-up session, choices of paired compared to non-paired items were related to enhanced BOLD activity in the precuneus and posterior cingulate cortex (PCC), which have been related to episodic memory retrieval and are also considered to be part of the default mode network (Cavanna & Trimble, 2006; Fransson & Marrelec, 2008; Sestieri, Corbetta, Romani, & Shulman, 2011; Shallice et al., 1994; Utevsky, Smith, & Huettel, 2014). This again demonstrates the central role of memory processes in the long-term behavioral change, as was shown in the relation between the change in hippocampal activity during passive viewing and the behavioral effect.

Individualized behavioral change

Overall, results obtained from the fMRI data during binary choices showed a similar pattern to those obtained during passive viewing: Enhanced perceptual processing in

the short-term and involvement of episodic memory processes in the long-term, as well as less involvement of top-down attention. We were not able to replicate previous results of enhanced activity in the vmPFC during choices of paired items, modulated by the number of choices of each item during probe (modulation across items) (Bakkour, Lewis-Peacock, et al., 2016; Schonberg et al., 2014). These previous results were found for high-value Go items when the group's behavioral effect of choosing high-value Go over high-value NoGo items was significant but weak relative to other samples (study 3 in Schonberg et al., 2014). Similar results were found for choices of low-value Go compared to choices of low-value NoGo items when the behavioral effect was strong for high-value items and weak for low-value items (Bakkour, Lewis-Peacock, et al., 2016). Therefore, a possible explanation for the lack of replication of these findings in the current study is that this contrast of modulation across items depends on the variance of the choice effect across items, which seems to be smaller here compared to previous samples that found this effect.

Related to this potential issue of variance is the fact that the CAT effect is a group effect. Not all participants choose paired over non-paired items following training, and there is a considerable variance across participants. In addition, training is performed on the individual item level, and thus preferences are affected only for some but not all paired items. The CAT effect in the one-month follow-up was relatively weak in the current study, although the behavioral effect was found to last for up to six months in previous studies (Salomon et al., 2018; Schonberg et al., 2014) . This might explain why our findings immediately after CAT were found in contrasts testing for main effects across all high-valued paired items, whereas results from the one-month follow-up were obtained mainly in parametric modulation of choices across items (within participants). Since the long-term behavioral effect was weaker than the effect in the

short-term, the variance across items was larger and enabled us to find differences in the response to different items in the follow-up session.

The long-term effect might have been relatively weaker than previous published work due to the new passive viewing task. In this task which was completed before, after and one month after training, items are presented on the screen without cues or motor responses, possibly resulting in partial extinction of the item-cue pairing established during training. In accordance with the marginally significant behavioral follow-up effect, the visual enhancement during passive viewing of paired compared to non-paired items was also present in the one-month follow-up (but only with $z>2.3$ threshold), but did not exceed statistical significance following cluster-based correction for multiple comparisons.

Our results suggest that in the short-term, perceptual processing is enhanced beyond all paired items, while in the long-term, the effect persists only for some of the items, and thus the overall behavioral effect is weaker and the neural changes are for specific items, these that elicited stronger response in memory-related regions, and not for all paired items. Furthermore, in the follow-up session we also found a negative correlation between the change of activity and the behavioral effect across participants (a group level correlation) in the parietal lobe. Since this correlation is not item-specific, but participant-specific, it informs us about the neural changes that were stronger for participants that were more affected by CAT, presumably the ones that were relying more on automatic processes, rather than top-down attention.

Suggested mechanism

Up until the current study it was not clear what is the mechanism underlying the CAT effect, unexplained by current value-based decision-making theories. How are

preferences represented in the brain and how can a simple non-reinforced training change them for a long period of time? Based on the findings of the current study, we suggest that low-level association-based paradigms, such as CAT, affect the neural representation of targeted individual items and draw bottom-up attention towards them, as manifested in previous studies with eye-gaze during binary choices (Schonberg et al., 2014) and probably less top-down attention (Veling et al., 2017). In the short-term, the enhanced bottom-up processing of individual paired items, leads to enhanced preferences towards them when a fast binary choice is required, mainly when there is less involvement of top-down attention. In the long-term, enhanced bottom-up perceptual processing and attention affected encoding and accessibility of these items in memory. During choices, positive associations in favor of the more accessible paired items accumulates faster to choices (Shadlen & Shohamy, 2016).

Conclusions

A previous influential review proposed a framework for studying the neurobiology of value-based decision-making (Rangel et al., 2008). They divided the decision-making process into five main computations: Representation, valuation, action selection, outcome evaluation and learning. Regarding the representation stage, they stated that “unfortunately, little is known about the computational and neurobiological basis of this step”. Previous research of the representation stage has mainly focused on reinforcement learning (e.g. Wilson & Niv, 2012). Our findings emphasize the importance of the representation stage and the necessity of studies investigating the representation of choice alternatives and its relation to preferences as well as the importance of memory in the short and long-term construction and modification of preferences (Shadlen & Shohamy, 2016; Weber & Johnson, 2006). Gaining

knowledge on the representation stage of decision-making and on non-reinforced change of preferences has great potential as a fruitful path for new theories relating neural mechanisms such as perceptual processing, memory and attention to preferences. It also holds great promise for new long-term behavioral change interventions based on automatic mechanisms, which might improve the quality of life for people around the world.

Methods

Data sharing. Behavioral data and codes are available at the Open Science Framework: https://osf.io/ts7b5/?view_only=c867c80179264ae5874af3d26ec39914. Imaging data is available in Brain Imaging Data Structure (BIDS) format (Gorgolewski et al., 2016) at OpenNeuro: https://openneuro.org/datasets/ds001417. Unthresholded statistical images are available at NeuroVault (Gorgolewski et al., 2015): https://neurovault.org/collections/TTZTGQNU/.

Participants. Forty healthy right-handed participants took part in this experiment. The sample size was chosen before data collection and pre-registered during data collection (https://osf.io/kxh9y/?view_only=4476c6fd74a84f0eb5a893df7e46700a). We initially planned to collect n = 35 participants based on previous imaging CAT samples and based on predicted 10% attrition for the one-month follow-up. However, during data collection we realized attrition rates are higher than expected, thus the planned sample size was increased to n = 40 (before exclusions and attrition), and re-pre-registered. The total number of participants included in the final analyses of the first session is 36 (19 females, age: mean = 26.11, SD = 3.46 years). Twenty-seven participants completed the follow up session (15 females, age: mean = 26.15, sd = 3.44 years).

Exclusions. A total of four participants were excluded: One participant due to incompletion of the experiment, one based on training exclusion criteria (7.5% false alarm rate during training) and two participants with incidental brain findings.

All participants had normal or corrected-to-normal vision and hearing, no history of eating disorders or psychiatric, neurologic or metabolic diagnoses, had no food restrictions and were not taking any medications that would interfere with the

experiment. They were asked to refrain from eating for four hours prior to arrival to the laboratory (Schonberg et al., 2014). All participants gave informed consent. The study was approved by the institutional review board at the Sheba Tel Hashomer Medical Center and the ethics committee at Tel Aviv University.

Stimuli: Sixty color images of familiar local snack food items were used in the current experiment. Images depicted the snack package and the snack itself on a homogenous black rectangle sized 576 x 432 pixels (see Supplementary Table 1; Stimuli dataset was created in our lab and is available online at http://schonberglab.tau.ac.il/resources/snack-food-image-database/). All snack food items were also available for actual consumption at the end of the experiment. Participants were presented with the real food items at the beginning of the experiment in order to promote incentive compatible behavior throughout the following tasks.

Experimental procedure: The general task procedure was similar to previous studies with CAT (Salomon et al., 2018; Schonberg et al., 2014). In order to test for functional changes of the neural response to the individual items following CAT, we added a new passive viewing task before, after and one month following training.

First, we obtained the subjective willingness to pay (WTP) of each participant for each of the 60 snack food items using a Becker-DeGroot-Marschak (BDM) auction procedure (Becker et al., 1964; Plassmann, O'Doherty, & Rangel, 2007), performed outside the MRI scanner (see Fig. 1a,g). Then, participants entered the scanner and completed two "passive viewing" runs while scanned with fMRI (see Fig. 1b,d), followed by anatomical and diffusion-weighted imaging (DWI) scans. Afterwards, participants went out of the scanner and completed cue-approach training (CAT) in a

behavioral testing room at the imaging center (see Fig. 1c). They then returned to the scanner and were scanned again with anatomical and DWI. Then, they were scanned with fMRI while performing two more runs of the “passive viewing” task and four runs of the probe phase, during which they chose between pairs of items (see Fig. 1e). Finally, participants completed a recognition task outside the scanner (see Fig. 1f), during which they were presented with snack items that appeared in previous parts of the experiment, as well as new items, and were asked to indicate for each item whether it was presented during the experiment and whether it was paired with the cue during training. As the last task during the first day of scanning, they again completed the BDM auction to obtain their WTP for the snacks.

Follow-up session. Approximately one month after the first day of the experiment, participants returned to the lab. They entered the scanner, were scanned with anatomical and DWI scans and completed two “passive viewing” runs as well as another probe phase (without additional training). Finally, participants completed the recognition and BDM auction parts, outside the scanner.

Anatomical and diffusion-weighted imaging data were obtained for each participant before, immediately after and one month following training. Analyses of diffusion data are beyond the scope of this paper.

Initial preferences evaluation (see Fig. 1a,g). In order to obtain initial subjective preferences, participants completed a BDM auction procedure (Becker et al., 1964; Plassmann et al., 2007). Participants first received 10 Israeli Shekels (ILS; equivalent to ~2.7$ US). During the auction, 60 snack food items were presented on the screen one after the other in random order. For each item, participants were asked to indicate their willingness to pay (WTP) for the presented item. Participants placed their bid for

each item using the mouse cursor along a visual analog scale, ranging from 0-10 ILS (task was self-paced). Participants were told in advance that at the end of the experiment, the computer will randomly generate a counter bid ranging between 0 - 10 ILS (with 0.5 increments) for one of the sixty items. If the bid placed by the participant exceeds the computer's bid, she or he will be required to buy the item for the computer's lower bid price. Otherwise, the participant will not be allowed to buy the snack but gets to retain the allocated 10 ILS. Participants were told that at the end of the experiment, they will stay in the room for 30 minutes and the only food they will be allowed to eat is the snack (in case they "won" the auction and purchased it). Participants were explicitly instructed that the best strategy for this task was to indicate their actual WTP for each item.

*Item selection***.** For each participant, items were rank ordered from 1 (highest value) to 60 (lowest value) based on their WTP. Then, 12 items (ranked 7-18) were defined as high-valued items to be used in probe, and 12 items (ranked 43-54) were defined as low-valued items to be used in probe. Each group of twelve items (high-value or low-value) was split to two sub groups with identical mean rank. Six of the 12 items were chosen to be paired with the cue during training (Go items; training procedures are described in the following sections), and the other six were not paired with the cue during training (NoGo items). This allowed us to pair high-value Go and high-value NoGo items, or low-value Go with low-value NoGo items, with similar initial WTPs, for the probe binary choices. To maintain 30% frequency of Go items during training (similar to previous studies with CAT; Bakkour, Leuker, et al., 2016; Bakkour, Lewis-Peacock, et al., 2016; Salomon et al., 2018; Schonberg et al., 2014), we used 16 additional NoGo items that were also used during training and passive viewing (40

snacks overall; see *Supplementary Fig. 1* for a detailed description of all stimuli allocation).

Passive viewing (*see Fig. 1b,d*). The task was performed inside the scanner, while participants were scanned with fMRI. This new task was introduced to evaluate the functional changes in the response to the individual items following CAT. The neural signature of the participants' response to each of the individual items was obtained in three different time points: A baseline measurement before CAT, after CAT and in a one-month follow-up. In this task, participants passively viewed a subset of 40 items, which were presented in the training procedure (see *item selection* section and *Supplementary Fig. 1*). The task consisted of two runs (in each session). On each run, each of the 40 items was presented on the screen for a fixed duration of two seconds, followed by a fixed inter-stimulus interval (ISI) of seven seconds. Items were presented in random order. To ensure participants were observing and processing the presented images, we asked them to perform a sham task of silently counting how many items were of snacks containing either one piece (e.g. a 'Mars' chocolate bar) or several pieces (e.g. a 'M&M' snack) in a new package. At the end of each run, participants were asked how many items they counted. Task instructions (count one / several) were counterbalanced between runs for each participant. The time elapsed between the two runs before training and two runs after training was about two hours (including cue-approach training, anatomical and diffusion weighted scans before and after training and time to exit and enter the scanner).

Cue-approach training (see *Fig. 1c*)**.** Training was performed outside the scanner. The training task included the same 40 items presented in the passive viewing task. Each image was presented on the screen one at a time for a fixed duration of one second.

Participants were instructed to press a button on the keyboard as fast as they could when they heard an auditory cue, which was consistently paired with 30% of the items (Go items). Participants were not informed in advance that some of the items will be consistently paired with the cue, or the identity of the Go items. The auditory cue consisted of a 180ms-long sinus wave function. The auditory cue was heard initially 750ms after stimulus onset (Go-signal delay, GSD). To ensure a success rate of around 75% in pressing the button before stimulus offset, we used a ladder technique to update the GSD. The GSD was increased by 16.67ms following every successful trial and decreased by 50ms if the participant did not press the button or pressed it after the offset of the stimulus (1:3 ratio). Items were followed by a fixation cross that appeared on the screen for a jittered ISI with an average duration of two seconds (range 1-6 seconds). Each participant completed 20 repetitions of training, each repetition included all 40 items presented in a random order. A short break was given following every two training repetitions, in which the participants were asked to press a button when they were ready to proceed. The entire training session lasted about 40-45 minutes, depending on the duration of the breaks, which were controlled by the participants.

Probe (see *Fig. 1e*). Probe was conducted while participants were scanned with fMRI. The probe phase was aimed to test participants' preferences following training. Participants were presented with pairs of items that had similar initial rankings (high-value or low-value), but only one of the items in each pair was associated with the cue during training (e.g. high-value Go vs. high-value NoGo). They were given 1.5 seconds to choose the item they preferred on each trial, by pressing one of two buttons on an MRI-compatible response box. Their choice was highlighted for 0.5 second with a

green rectangle around the chosen items. If they did not respond on time, a message appeared on the screen, asking them to respond faster. A fixation cross appeared at the center of the screen between the two items during each trial, as well as during the ISI, which lasted on average three seconds (range 1-12 seconds).

The probe phase consisted of two blocks. On each block, each of the six high-value Go items were compared with each of the six high-value NoGo items (36 comparisons), as well as each of the six low-value Go items with each of the six low-value NoGo items. Thus, overall there were 72 pairs of Go-NoGo comparisons (each repeated twice during probe, once on each block). In addition, on each block we compared each of two high-value NoGo items versus each of two low-value NoGo items, resulting in four probe pairs that were used as “sanity checks” to ensure participants chose the items they preferred according to the initial WTP values obtained during the BDM auction. Each probe block was divided to two runs, each consisted of half of the total 76 unique pairs (38 trials on each run). All pairs within each run were presented in a random order, and the location of the items (left/right) was also randomly chosen. Choices during the probe phase were made for consumption to ensure they were incentive-compatible. Participants were told that a single trial will be randomly chosen at the end of the experiment and that they will receive the item they chose on that specific trial. The participants were shown the snack box with all snacks prior to the beginning of the experiment.

Recognition (see *Fig. 1f*). Participants completed a recognition task, were the items from the probe phase, as well as new items, were presented on the screen one by one and they were asked to indicate for each item whether or not it was presented during

the experiment and whether or not it was paired with the cue during training. Analysis of this task is beyond the scope of this paper.

One-month follow–up session. All participants were invited to the follow-up session approximately one month after training. A subset of 27participants returned to the lab and completed the follow-up session. They were scanned with anatomical and diffusion protocols, completed two passive viewing runs and performed another probe while scanned with fMRI protocols, similar to the first session. In the follow-up session, the probe included the same pairs as the probe of the first session, presented in a new random order. Afterwards, participants completed another session of the recognition task and a third BDM auction, both outside the scanner in the testing room.

Behavioral analysis of the probe phase. Similar to previous studies using cue-approach task (Salomon et al., 2018; Schonberg et al., 2014), we performed a repeated-measures logistic regression to compare the odds of choosing Go items against chance level (log-odds = 0; odds ratio = 1) for each trial type (high-value / low-value). We also compared the ratio of choosing the Go items between high-value and low-value pairs. These analyses were conducted for each session separately.

MRI acquisition. Imaging data were acquired using a 3T Siemens Prisma MRI scanner with a 64-channel head coil, at the Strauss imaging center on the campus of Tel Aviv University. Functional data were acquired using a T2*-weighted echo planer imaging sequence. Repetition time (TR) = 2000ms, echo time (TE) = 30ms, flip angle (FA) = 90°, field of view (FOV) = 224 × 224mm, acquisition matrix of 112 × 112. We positioned 58 oblique axial slices with a 2 × 2mm in plane resolution 15° off the anterior

commissure-posterior commissure line to reduce the frontal signal dropout (Deichmann, Gottfried, Hutton, & Turner, 2003), with a space of 2mm and a gap of 0.5mm to cover the entire brain. We used a multiband sequence (Moeller et al., 2010) with acceleration factor = 2 and parallel imaging factor (iPAT) = 2, in an interleaved fashion. Each of the passive viewing runs consisted of 180 volumes and each of the probe runs consisted of 100 volumes. In addition, in each scanning session (before, after and one month following training) we acquired high-resolution T1w structural images using a magnetization prepared rapid gradient echo (MPRAGE) pulse sequence (TR = 1.75s, TE = 2.59ms, FA = 8°, FOV = 224 × 224 × 208mm, resolution = 1 × 1 × 1mm for the first five participants; TR = 2.53s, TE = 2.88ms, FA = 7°, FOV = 224 × 224 × 208mm, resolution = 1 × 1 × 1mm for the rest of the sample. Protocol was changed to enhance the T1w contrast and improve registration of the functional data to the standard space).

fMRI preprocessing: Raw imaging data in DICOM format were converted to NIfTI format with dcm2nii tool (Li, Morgan, Ashburner, Smith, & Rorden, 2016). The NIfTI files were organized according to the Brain Imaging Data Structure (BIDS) format v1.0.1 (K. J. Gorgolewski et al., 2016). Preprocessing of the functional imaging data was performed using fMRIprep version 1.0.0-rc8 (Esteban et al., 2018), a Nipype (K. Gorgolewski et al., 2011; Gorgolewski KJ, Esteban O, Ellis DG, Notter MP, Ziegler E, Johnson H, Hamalainen C, Yvernault B, Burns C, Manhães-Savio A, Jarecka D, Markiewicz CJ, Salo T, Clark D, Waskom M, Wong J, Modat M, Dewey BE, Clark MG, Dayan M, Loney F, Madison C, Gramfort A, K, 2017) based tool. Each T1 weighted volume was corrected for bias field using N4BiasFieldCorrection v2.1.0 (Tustison et al., 2010) and skull stripped using antsBrainExtraction.sh v2.1.0 (using

OASIS template). Cortical surface was estimated using FreeSurfer v6.0.0 (Dale, Fischl, & Sereno, 1999). The skull stripped T1 weighted volume was coregistered to skull stripped ICBM 152 Nonlinear template version 2009c (Fonov VS, Evans AC, McKinstry RC, Almli CR, 2009) using nonlinear transformation implemented in ANTs v2.1.0 (Avants, Epstein, Grossman, & Gee, 2008). Functional data were motion corrected using MCFLIRT v5.0.9 (Jenkinson, Bannister, Brady, & Smith, 2002). This was followed by co-registration to the corresponding T1 weighted volume using boundary based registration with nine degrees of freedom, implemented in FreeSurfer v6.0.0 (Greve & Fischl, 2009). Motion correcting transformations, T1 weighted transformation and MNI template warp were applied in a single step using antsApplyTransformations v2.1.0 with Lanczos interpolation. Three tissue classes were extracted from the T1 weighted images using FSL FAST v5.0.9 (Zhang, Brady, & Smith, 2001). Voxels from cerebrospinal fluid and white matter were used to create a mask in turn used to extract physiological noise regressors using aCompCor (Behzadi, 2008). Mask was eroded and limited to subcortical regions to limit overlap with grey matter, and six principal components were estimated. Framewise displacements (Power et al., 2014) was calculated for each functional run using Nipype implementation. For more details of the pipeline using fMRIprep see http://fmriprep.readthedocs.io/en/1.0.0-rc8/workflows.html. We created confound files (tsv format) for each scan (each run of each task of each session of each participant), with the following columns: standard deviation of the root mean squared (RMS) intensity difference from one volume to the next (DVARS), absolute DVARS values, voxelwise standard deviation of DVARS values and six motion parameters (translational and rotation, each in three directions). We added a single time point regressor (a single additional column) for each volume with framewise-displacement

value larger than 0.9, in order to model out volumes with extensive motion. Scans with more than 15% scrubbed volumes were excluded from analysis, resulting in one excluded participant from the analysis of the first session's probe task.

fMRI analysis. Imaging analysis was performed using FEAT (fMRI Expert Analysis Tool) v6.00, part of FSL (FMRIB's Software Library) v5.0.10 (Smith et al., 2004).

Univariate imaging analysis - passive viewing: The functional data from the passive viewing task were used to examine the functional changes underlying the behavioral change of preferences following CAT in the short and long-term. We used a general linear model (GLM) with 13 regressors: Six regressors modelling each item type (high-value Go, high-value NoGo, high-value sanity, low-value Go, low-value NoGo and low-value sanity); six regressors with the same onsets and duration, and a parametric modulation by the mean-centered proportion of trials each item was chosen in the subsequent probe phase (the number of trials each item was chosen during the subsequent probe divided by the number of probe trials including this item, mean-centered) and one regressor for all items with a parametric modulation by the mean-centered WTP values acquired from the first BDM auction. These 13 regressors were convolved with the canonical double-gamma hemodynamic response function, and their temporal derivatives were added to the model. We further included at least nine motion regressors as confounds, as described above. We estimated a model with the above described GLM regressors for each passive viewing run of each participant in a first level analysis.

In the second level analysis (fixed effects), runs from the same session were averaged and compared to the other session. Two second level contrasts were analyzed separately: after compared to before CAT and follow-up compared to before CAT.

All second level analyses of all participants from after minus before or from follow-up minus before CAT were then inputted to a group level analysis (mixed effects), which included two contrasts of interest: One with the main effect (indicating group mean) and one with the mean centered probe effect of each participant (the demeaned proportion of choosing Go over NoGo items during the subsequent probe in the relevant pair type, i.e. either high-value, low-value or all probe pairs). The second contrast was used to test the correlation between the fMRI activations and the behavioral effect across participants (correlation with the behavioral effect across participants).

All reported group level statistical maps were thresholded at Z > 2.3 and cluster-based Gaussian Random Field corrected for multiple comparisons at the whole-brain level with a (corrected) cluster significance threshold of $P = 0.05$ (Worsley, 2001).

Since we only found a behavioral effect for high-value items, similarly to previous cue-approach samples with snack food items (Salomon et al., 2018; Schonberg et al., 2014), we focused our analyses on the contrasts for high-value items: high-value Go items, high-value Go items modulated by choice and high-value Go minus high-value NoGo items.

Univariate imaging analysis - probe: Imaging analysis of the probe data was similar to previous imaging studies with CAT (Bakkour, Lewis-Peacock, et al., 2016; Schonberg et al., 2014). We included 16 regressors in the model (in addition to at least nine motion regressors), based on the initial value of the probe pair (high / low) and the choice outcome (participant chose the Go / NoGo item), resulting in four regressors (high-value chose Go / high-value chose NoGo / low-value chose Go / low-value chose NoGo) without parametric modulation; the same four regressors with a parametric

modulation across items by the mean-centered proportion of choices of the specific item during the entire probe phase; the same four regressors with a parametric modulation by the WTP difference between the two presented items; one regressor for all “sanity-check” trials; one regressor for all missed trials; and two regressors accounting for response time differences (one regressor with a modulation of the demeaned response time across trials for each value category).

Since our behavioral effect was stronger for high-value items (similar to previous cue-approach samples with snack food items), we focused our analysis on the contrasts for high-value chose Go, high-value chose Go modulated by choice and high-value chose Go minus high-value chose NoGo. Similar to analyses of the passive viewing task, we estimated a first level GLM for each run of each participant. We then averaged the four runs of each probe (after / follow-up) of each participant in a second-level analysis. Finally, we ran a group level analysis as described above, with one contrast for the mean group effect and one contrast for the demeaned probe effect across participants (correlation with the behavioral effect across participants).

Some of the probe runs were excluded from the imaging analysis (i.e. not included in the second level analysis of the specific participant) because one of the regressors was empty or because the parametric modulator of Go item choices was zeroed out, resulting in a rank-deficient design matrix. This happened, for example, when a participant chose high-value Go over high-value NoGo items on all trials of a specific run. Participants who did not have at least one full valid block (out of two probe blocks, each probe including one presentation of each probe pair) without any empty regressors or zeroed modulators for Go items, were excluded from the probe imaging analysis. In order to minimize the number of excluded runs and participants, we did not exclude runs or participants due to a zeroed modulator of NoGo items choices, but

rather decided not to use the contrasts including modulation by choice of trials where NoGo items were chosen. Overall, one participant was excluded from the imaging analysis of the probe from both the after and follow-up sessions and two more were excluded each from one of the sessions, based on regressors causing rank-deficient matrices (in addition to the one participant that was excluded from the first session due to excessive motion, as described above). Thus, a total of 33 (out of 36) participants were included in the imaging analysis of the probe after training (out of which for 28 participants no run was excluded, for four participants one run was excluded and for one participants two runs- one block- were excluded), and 25 (out of 27) participants were included in the imaging analysis of the follow-up probe (out of which for 21 participants no run was excluded and for four participants one run was excluded).

<u>Small volume correction (SVC) analysis - passive viewing:</u> We pre-hypothesized (and pre-registered) that value, attention and memory-related regions will be involved in the behavioral change following CAT: Prefrontal cortex, dorsal parietal cortex and medial-temporal lobe, respectively (https://osf.io/6mysj/). Thus, in addition to the whole-brain analyses described above for the passive viewing and probe task, we ran similar group level analyses once for each of these pre-hypothesized regions (bilateral hippocampus, bilateral SPL and vmPFC), with a mask containing the voxels which were part of the region. All masks were based on the Harvard-Oxford atlas (see *Supplementary Fig. 2*), anatomical regions for the vmPFC mask were based on those used in previous CAT papers (Bakkour, Lewis-Peacock, et al., 2016; Schonberg et al., 2014).

Pre-registration of analysis plan. Our analysis plan was pre-registered (https://osf.io/x6hsq/?view_only=d3d59209e1704f97bc044b7aa6eb6fd2) prior to final full analyses.

Acknowledgements

We thank Dr. Jeanette Mumford for her invaluable statistics advices. This research was supported by a grant from the Israel Science Foundation (ISF; grant no. 1798/15) granted to Tom Schonberg.

Author contributions

R.B.N. and T.Sc. designed the experiment, R.B.N. and T.Sa. collected the data, R.B.N., T.Sa. and T.Sc analyzed the data, discussed the results and wrote the paper.

REFERENCES

Avants, B. B., Epstein, C. L., Grossman, M., & Gee, J. C. (2008). Symmetric diffeomorphic image registration with cross-correlation: Evaluating automated labeling of elderly and neurodegenerative brain. *Medical Image Analysis*, *12*(1), 26–41. https://doi.org/10.1016/j.media.2007.06.004

Bakkour, A., Leuker, C., Hover, A. M., Giles, N., Poldrack, R. A., & Schonberg, T. (2016). Mechanisms of Choice Behavior Shift Using Cue-approach Training. *Frontiers in Psychology*, *7*(March), 1–12. https://doi.org/10.3389/fpsyg.2016.00421

Bakkour, A., Lewis-Peacock, J. A., Poldrack, R. A., & Schonberg, T. (2016). Neural mechanisms of cue-approach training. *NeuroImage*, (September), 0–1. https://doi.org/10.1016/j.neuroimage.2016.09.059

Balleine, B. W. (2005). Neural bases of food-seeking: Affect, arousal and reward in corticostriatolimbic circuits. *Physiology and Behavior*, *86*(5), 717–730. https://doi.org/10.1016/j.physbeh.2005.08.061

Balleine, B. W., & O'Doherty, J. P. (2010). Human and rodent homologies in action control: corticostriatal determinants of goal-directed and habitual action. *Neuropsychopharmacology : Official Publication of the American College of Neuropsychopharmacology*, *35*(1), 48–69. https://doi.org/10.1038/npp.2009.131

Becker, G. M., DeGroot, M. H., & Marschak, J. (1964). Measuring utility by a single-response sequential method. *Behavioral Science*, *9*(3), 226–232. https://doi.org/10.1002/bs.3830090304

Behzadi. (2008). A Component Based Noise Correction Method (CompCor) for BOLD and Perfusion Based fMRI, *37*(1), 90–101.

Cai, X., Kim, S., & Lee, D. (2011). Heterogeneous Coding of Temporally Discounted Values in the Dorsal and Ventral Striatum during Intertemporal Choice. *Neuron*, *69*(1), 170–182. https://doi.org/10.1016/j.neuron.2010.11.041

Cai, X., & Padoa-Schioppa, C. (2014). Contributions of orbitofrontal and lateral prefrontal cortices to economic choice and the good-to-action transformation. *Neuron*, *81*(5), 1140–1151. https://doi.org/10.1016/j.neuron.2014.01.008

Cavanna, A. E., & Trimble, M. R. (2006). The precuneus: A review of its functional anatomy and behavioural correlates. *Brain*, *129*(3), 564–583. https://doi.org/10.1093/brain/awl004

Christiansen, T., Bruun, J. M., Madsen, E. L., & Richelsen, B. (2007). Weight loss maintenance in severely obese adults after an intensive lifestyle intervention: 2- to 4-year follow-up. *Obesity (Silver Spring, Md.)*, *15*(2), 413–420. https://doi.org/10.1038/oby.2007.530

Culham, J. C., & Kanwisher, N. G. (2001). Neuroimaging of cognitive functions in human parietal cortex. *Current Opinion in Neurobiology*, *11*(2), 157–163. https://doi.org/10.1016/S0959-4388(00)00191-4

Dale, A. M., Fischl, B., & Sereno, M. I. (1999). Cortical surface-based analysis: I. Segmentation and surface reconstruction. *NeuroImage*, *9*(2), 179–194. https://doi.org/10.1006/nimg.1998.0395

Daniel, R., & Pollmann, S. (2014). A universal role of the ventral striatum in reward-based learning: Evidence from human studies. *Neurobiology of Learning and Memory*, *114*, 90–100. https://doi.org/10.1016/j.nlm.2014.05.002

Deichmann, R., Gottfried, J. a., Hutton, C., & Turner, R. (2003). Optimized EPI for fMRI studies of the orbitofrontal cortex. *NeuroImage*, *19*(2), 430–441.

https://doi.org/10.1016/S1053-8119(03)00073-9
Esteban, O., Blair, R., Markiewicz, C. J., Berleant, S. L., Moodie, C., Ma, F., … Gorgolewski, K. J. (2018). poldracklab/fmriprep: 1.0.8. https://doi.org/10.5281/ZENODO.1183390
Fonov VS, Evans AC, McKinstry RC, Almli CR, C. D. (2009). Unbiased nonlinear average age-appropriate brain templates from birth to adulthood. https://doi.org/10.1016/S1053-8119(09)70884-5
Fransson, P., & Marrelec, G. (2008). The precuneus/posterior cingulate cortex plays a pivotal role in the default mode network: Evidence from a partial correlation network analysis. *NeuroImage*, *42*(3), 1178–1184. https://doi.org/10.1016/j.neuroimage.2008.05.059
Goodale, M. a., & Milner, a. D. (1992). Separate visual pathways for perception and action. [Review] [61 refs]. *Trends in Neurosciences*, *15*(I), 20–25. https://doi.org/10.1016/0166-2236(92)90344-8
Gorgolewski, K., Burns, C. D., Madison, C., Clark, D., Halchenko, Y. O., Waskom, M. L., & Ghosh, S. S. (2011). Nipype: A Flexible, Lightweight and Extensible Neuroimaging Data Processing Framework in Python. *Frontiers in Neuroinformatics*, *5*(August). https://doi.org/10.3389/fninf.2011.00013
Gorgolewski, K. J., Auer, T., Calhoun, V. D., Craddock, R. C., Das, S., Duff, E. P., … Poldrack, R. A. (2016). The brain imaging data structure, a format for organizing and describing outputs of neuroimaging experiments. *Scientific Data*, *3*, 1–9. https://doi.org/10.1038/sdata.2016.44
Gorgolewski, K. J., Varoquaux, G., Rivera, G., Schwarz, Y., Ghosh, S. S., Maumet, C., … Margulies, D. S. (2015). NeuroVault.org: a web-based repository for collecting and sharing unthresholded statistical maps of the human brain. *Frontiers in Neuroinformatics*, *9*(April), 1–9. https://doi.org/10.3389/fninf.2015.00008
Gorgolewski KJ, Esteban O, Ellis DG, Notter MP, Ziegler E, Johnson H, Hamalainen C, Yvernault B, Burns C, Manhães-Savio A, Jarecka D, Markiewicz CJ, Salo T, Clark D, Waskom M, Wong J, Modat M, Dewey BE, Clark MG, Dayan M, Loney F, Madison C, Gramfort A, K, G. S. (2017). Nipype: a flexible, lightweight and extensible neuroimaging data processing framework in Python. https://doi.org/10.5281/zenodo.596855
Greve, D. N., & Fischl, B. (2009). Accurate and robust brain image alignment using boundary-based registration. *NeuroImage*, *48*(1), 63–72. https://doi.org/10.1016/j.neuroimage.2009.06.060
Grill-Spector, K. (2003). The neural basis of object perception. *Current Opinion in Neurobiology*, *13*(2), 159–166. https://doi.org/10.1016/S0959-4388(03)00040-0
Grill-Spector, K., Kourtzi, Z., & Kanwisher, N. (2001). The lateral occipital complex and its role in object recognition. *Vision Research*, *41*(10–11), 1409–1422. https://doi.org/10.1016/S0042-6989(01)00073-6
Ishai, a, Ungerleider, L. G., Martin, a, & Haxby, J. V. (2000). The representation of objects in the human occipital and temporal cortex. *Journal of Cognitive Neuroscience*, *12 Suppl 2*, 35–51. https://doi.org/10.1162/089892900564055
Jeffery, R. W., Drewnowski, a, Epstein, L. H., Stunkard, a J., Wilson, G. T., Wing, R. R., & Hill, D. R. (2000). Long-term maintenance of weight loss: current status. *Health Psychology : Official Journal of the Division of Health Psychology, American Psychological Association*, *19*(1 Suppl), 5–16. https://doi.org/10.1037//0278-6133.19.1(Suppl.).5
Jenkinson, M., Bannister, P., Brady, M., & Smith, S. (2002). Improved optimization

for the robust and accurate linear registration and motion correction of brain images. *NeuroImage*, *17*(2), 825–841. https://doi.org/10.1016/S1053-8119(02)91132-8

Kable, J. W., & Glimcher, P. W. (2009). The Neurobiology of Decision: Consensus and Controversy. *Neuron*, *63*(6), 733–745. https://doi.org/10.1016/j.neuron.2009.09.003

Lebreton, M., Jorge, S., Michel, V., Thirion, B., & Pessiglione, M. (2009). An Automatic Valuation System in the Human Brain: Evidence from Functional Neuroimaging. *Neuron*, *64*(3), 431–439. https://doi.org/10.1016/j.neuron.2009.09.040

Levy, D. J., & Glimcher, P. W. (2012). The root of all value: a neural common currency for choice. *Current Opinion in Neurobiology*, *22*(6), 1027–1038. https://doi.org/10.1016/j.conb.2012.06.001

Levy, I., Lazzaro, S. C., Rutledge, R. B., & Glimcher, P. W. (2011). Choice from Non-Choice: Predicting Consumer Preferences from Blood Oxygenation Level-Dependent Signals Obtained during Passive Viewing. *Journal of Neuroscience*, *31*(1), 118–125. https://doi.org/10.1523/JNEUROSCI.3214-10.2011

Li, X., Morgan, P. S., Ashburner, J., Smith, J., & Rorden, C. (2016). The first step for neuroimaging data analysis: DICOM to NIfTI conversion. *Journal of Neuroscience Methods*, *264*, 47–56. https://doi.org/10.1016/j.jneumeth.2016.03.001

Marteau, T. M., Hollands, G. J., & Fletcher, P. C. (2012). Changing Human Behavior to Prevent Disease: The Importance of Targeting Automatic Processes. *Science*, *337*, 1492–1495. https://doi.org/10.1126/science.1226918

Martino, B. De, Kumaran, D., Seymour, B., & Dolan, R. J. (2006). Decision-Making in the Human Brain, (August), 684–688.

Moeller, S., Yacoub, E., Olman, C. a., Auerbach, E., Strupp, J., Harel, N., & Uğurbil, K. (2010). Multiband multislice GE-EPI at 7 tesla, with 16-fold acceleration using partial parallel imaging with application to high spatial and temporal whole-brain FMRI. *Magnetic Resonance in Medicine*, *63*(5), 1144–1153. https://doi.org/10.1002/mrm.22361

Padoa-Schioppa, C. (2011). Neurobiology of Economic Choice: A Good-Based Model. *Annual Review of Neuroscience*, *34*(1), 333–359. https://doi.org/10.1146/annurev-neuro-061010-113648

Padoa-Schioppa, C., & Cai, X. (2011). The orbitofrontal cortex and the computation of subjective value: Consolidated concepts and new perspectives. *Annals of the New York Academy of Sciences*, *1239*(1), 130–137. https://doi.org/10.1111/j.1749-6632.2011.06262.x

Plassmann, H., O'Doherty, J., & Rangel, A. (2007). Orbitofrontal cortex encodes willingness to pay in everyday economic transactions. *The Journal of Neuroscience : The Official Journal of the Society for Neuroscience*, *27*(37), 9984–9988. https://doi.org/10.1523/JNEUROSCI.2131-07.2007

Power, J. D., Mitra, A., Laumann, T. O., Snyder, A. Z., Schlaggar, B. L., & Petersen, S. E. (2014). Methods to detect, characterize, and remove motion artifact in resting state fMRI. *NeuroImage*, *84*, 320–341. https://doi.org/10.1016/j.neuroimage.2013.08.048

Prochaska, J. J., Delucchi, K., & Hall, S. M. (2004). A meta-analysis of smoking cessation interventions with individuals in substance abuse treatment or recovery. *Journal of Consulting and Clinical Psychology*, *72*(6), 1144–1156. https://doi.org/10.1037/0022-006X.72.6.1144

Rangel, A., Camerer, C., & Montague, P. R. (2008). A framework for studying the neurobiology of value-based decision making. *Nature Reviews. Neuroscience*, *9*(july), 545–556. https://doi.org/10.1038/nrn2357

Salomon, T., Botvinik-Nezer, R., Gutentag, T., Gera, R., Iwanir, R., Tamir, M., & Schonberg, T. (2018). The Cue-Approach Task as a General Mechanism for Long-Term Non-Reinforced Behavioral Change. *Scientific Reports*, *8*(1), 3614. https://doi.org/10.1038/s41598-018-21774-3

Schonberg, T., Bakkour, A., hleigh M, Mumford, J. a, Nagar, L., Perez, J., & Poldrack, R. a. (2014). Changing value through cued approach: an automatic mechanism of behavior change. *Nature Neuroscience*, *17*(4), 625–630. https://doi.org/10.1038/nn.3673

Serences, J. T. (2008). Value-Based Modulations in Human Visual Cortex. *Neuron*, *60*(6), 1169–1181. https://doi.org/10.1016/j.neuron.2008.10.051

Sestieri, C., Corbetta, M., Romani, G. L., & Shulman, G. L. (2011). Episodic Memory Retrieval, Parietal Cortex, and the Default Mode Network: Functional and Topographic Analyses. *Journal of Neuroscience*, *31*(12), 4407–4420. https://doi.org/10.1523/JNEUROSCI.3335-10.2011

Shadlen, M. N., & Shohamy, D. (2016). Decision Making and Sequential Sampling from Memory. *Neuron*, *90*(5), 927–939. https://doi.org/10.1016/j.neuron.2016.04.036

Shallice, T., Fletcher, P., Frith, C. D., Grasby, P., Frackowiak, R. S., & Dolan, R. J. (1994). Brain regions associated with acquisition and retrieval of verbal episodic memory. *Nature*, *368*(6472), 633–635. https://doi.org/10.1038/368633a0

Smith, S. M., Jenkinson, M., Woolrich, M. W., Beckmann, C. F., Behrens, T. E. J., Johansen-Berg, H., … Matthews, P. M. (2004). Advances in functional and structural MR image analysis and implementation as FSL. *NeuroImage*, *23*(SUPPL. 1), 208–219. https://doi.org/10.1016/j.neuroimage.2004.07.051

Tustison, N. J., Avants, B. B., Cook, P. A., Zheng, Y., Egan, A., Yushkevich, P. A., & Gee, J. C. (2010). N4ITK: Improved N3 bias correction. *IEEE Transactions on Medical Imaging*, *29*(6), 1310–1320. https://doi.org/10.1109/TMI.2010.2046908

Tversky, A., & Kahneman, D. (1986). Rational Choice and the Framing of Decisions The Journal of Business , Vol . 59 , No . 4 , Part 2 : The Behavioral Foundations of Economic Theory (Oct ., 1986), pp . S251-S278

Utevsky, A. V., Smith, D. V., & Huettel, S. A. (2014). Precuneus Is a Functional Core of the Default-Mode Network. *The Journal of Neuroscience*, *34*(3), 932–940. https://doi.org/10.1523/JNEUROSCI.4227-13.2014

Veling, H., Chen, Z., Tombrock, M. C., Verpaalen, I. A. M., Schmitz, L. I., Dijksterhuis, A., & Holland, R. W. (2017). Training impulsive choices for healthy and sustainable food. *Journal of Experimental Psychology: Applied*, *23*(2), 204–215. https://doi.org/10.1037/xap0000112

Vlaev, I., Chater, N., Stewart, N., & Brown, G. D. a. (2011). Does the brain calculate value? *Trends in Cognitive Sciences*, *15*(11), 546–554. https://doi.org/10.1016/j.tics.2011.09.008

Weber, E. U., & Johnson, E. J. (2006). Constructing Preferences from Memory. *SSRN Electronic Journal*, 1–26. https://doi.org/10.2139/ssrn.1301075

Wilson, R. C., & Niv, Y. (2012). Inferring Relevance in a Changing World. *Frontiers in Human Neuroscience*, *5* (January), 1–14. https://doi.org/10.3389/fnhum.2011.00189

Worsley, K. J. (2001). Functional MRI: An introduction to methods. *Functional MRI: An Introduction to Methods*, 251–270. https://doi.org/10.1093/acprof

Yin, H. H., & Knowlton, B. J. (2006). The role of the basal ganglia in habit formation. *Nature Reviews Neuroscience*, *7*(6), 464–476. https://doi.org/10.1038/nrn1919

Zhang, Y., Brady, M., & Smith, S. (2001). Segmentation of brain MR images through a hidden Markov random field model and the expectation-maximization algorithm. *IEEE Transactions on Medical Imaging*, *20*(1), 45–57. https://doi.org/10.1109/42.906424

Zoltak, M. J., Veling, H., Chen, Z., & Holland, R. W. (2017). Attention! Can choices for low value food over high value food be trained? *Appetite*, *124*, 124–132. https://doi.org/10.1016/j.appet.2017.06.010

Supplementary data: Eye-tracking

Eye-tracking data were recorded from a subset of participants, using an EyeLink 1000 Plus SR-Research eye-tracker. For the passive viewing task, we had useable eye-gaze data from 10 participants after CAT and 10 participants in the one-month follow-up (we did not obtain eye-tracking data prior to training). Eye-tracking data from the passive viewing task were used to test whether the duration of time spent observing Go items was different from the duration observing NoGo items after CAT. We averaged the time spent looking on Go items and the time spent looking on NoGo items for each participant and performed a paired t-test to test for differences in observation time between Go and NoGo items.

We found no differences in eye-gaze duration between high-value Go and NoGo items during the task, neither after CAT (mean percent of viewing time: high-value Go 75.3%, high-value NoGo 77.4%; $P = 0.512$) nor in the follow-up session (mean percent of viewing time: high-value Go 77.9%, high-value NoGo 74.2%; $P = 0.266$).

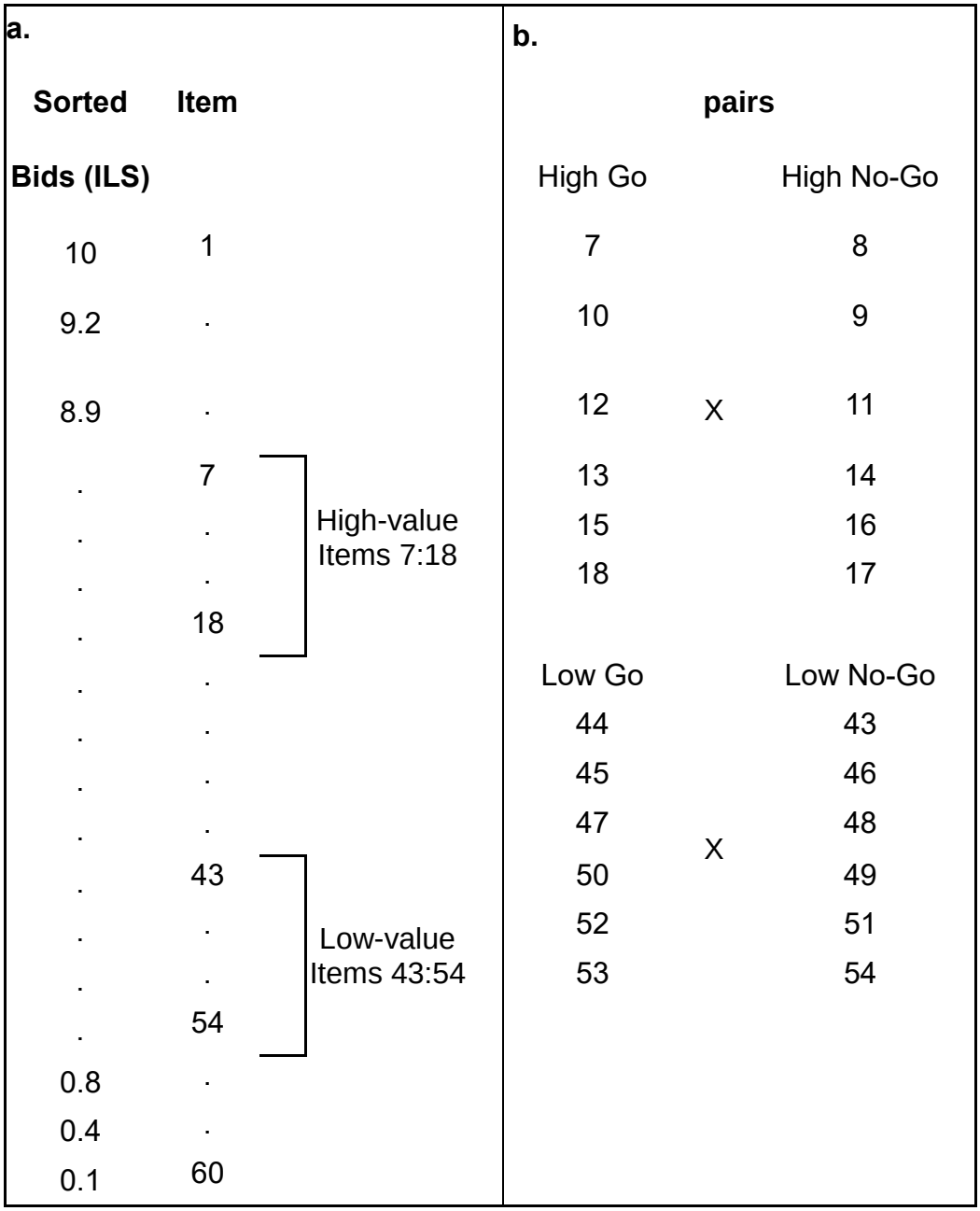

Supplementary Figure 1. *Diagram of the item selection procedure used in this study.*

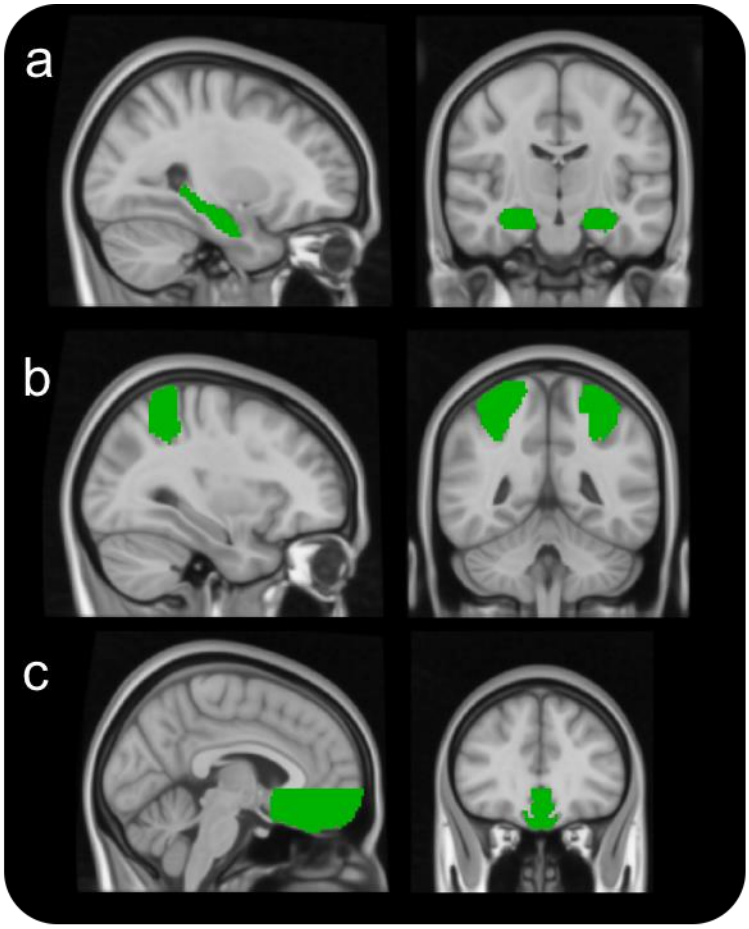

Supplementary Figure 2. *Masks for small volume correction: (a) Left and right hippocampus; (b) left and right SPL; (c) vmPFC.*

	Brand	Description		Brand	Description
1	Apropo	Salty snack	**31**	GumiWine	Gummy candy
2	BabyDoll	Candy	**32**	Halva	Halva
3	BagaleShtuhim	Salty snack	**33**	HappyHippo	Chocolate
4	Bamba	Salty snack	**34**	HispusimShatiah	Gummy candy
5	BambaNugat	Sweet and salty snack	**35**	Hit	Cookies
6	BambaSweet	Sweet and salty snack	**36**	KashitSour	Gummy candy
7	BisliBbq	Salty snack	**37**	Keifli	Salty snack
8	BisliGrill	Salty snack	**38**	KifkefMaklot	Chocolate
9	BisliOnion	Salty snack	**39**	KinderBuenoBrown	Chocolate
10	BisliPizza	Salty snack	**40**	KinderBuenoWhite	Chocolate
11	Bounty	Chocolate	**41**	KinderJoy	Chocolate
12	Cheetos	Salty snack	**42**	Kitkat	Chocolate
13	ChocolateParaCookies	Chocolate	**43**	Loacker	Wafer
14	ChocolateParaMarir	Chocolate	**44**	Mars	Chocolate
15	ChocolateParaMilk	Chocolate	**45**	Mekupelet	Chocolate
16	ChocolateParaSucariot	Chocolate	**46**	Mentos	Candy
17	ClickBalls	Chocolate	**47**	PesekZman	Chocolate
18	ClickBisquit	Chocolate	**48**	Popco	Sweet and salty snack
19	ClickBlackWhite	Chocolate	**49**	Shugi	Energy bar
20	ClickXLbrown	Chocolate	**50**	SkittlesFruits	Candy
21	ClickXLwhite	Chocolate	**51**	SkittlesSour	Candy
22	CrunchBisquitBrown	Chocolate	**52**	Smarties	Candy
23	CrunchBisquitWhite	Chocolate	**53**	Snickers	Chocolate
24	CrunchShokoVanil	Chocolate	**54**	Taami	Chocolate
25	DoritosGrill	Salty snack	**55**	Tapuchips	Salty snack
26	DoritosNatural	Salty snack	**56**	Tictac	Candy
27	DoritosSourSpicy	Salty snack	**57**	Tortit	Chocolate
28	Dubonim	Salty snack	**58**	Twist	Wafer
29	Egozi	Chocolate	**59**	Twix	Wafer
30	GumiSnakes	Gummy candy	**60**	WerthersOriginal	Candy

Supplementary Table 1. *Snack food stimuli used in this study.*

The complete images data set is available online:

http://schonberglab.tau.ac.il/resources/snack-food-image-database/

Contrast	Cluster	Region	Number of voxels in region	Cluster size	X	Y	Z	Peak z stat
High-value Go minus NoGo (Fig. 3a)	1	L Lateral Occipital Cortex, inferior division	104	171	-44	-72	-11	4
		L Inferior Temporal Gyrus, temporooccipital part	38					
		L Temporal Occipital Fusiform Cortex	19					
	2	R Temporal Occipital Fusiform Cortex	107	192	30	-46	-8	3.82
		R Lingual Gyrus	33					
		R Occipital Fusiform Gyrus	22					
		R Lateral Occipital Cortex, inferior division	20					
High-value Go, small volume correction (vmPFC; Fig. 3b)	1	L Frontal Medial Cortex	50	98	-10	48	-11	3.44
		R Frontal Medial Cortex	33					

***Supplementary Table 2**. Passive viewing task, after minus before CAT: Regions with significant activation for the imaging contrasts of **Fig. 3**. For each cluster, the list presents all regions from the Harvard-Oxford atlas that contained at least 10 active voxels within the cluster, as well as the X/Y/Z location for the peak activation in MNI space.*

Contrast	Cluster	Region	Number of voxels in region	Cluster size	X	Y	Z	Peak z stat
High-value Go, small volume correction (vmPFC; Fig. 4a)	1	R Frontal Medial Cortex	24	58	2	56	-18	3.21
		L Frontal Medial Cortex	23					
		R Frontal Pole	10					
High-value Go, modulation across items (Fig. 4b)	1	L Frontal Pole	140	147	-28	46	-15.5	3.59
High-value Go, modulation across items, small volume correction (hippocampus; Fig. 4c)	1	Right Hippocampus	34	36	26	-6	-25.5	3.79
High-value Go minus NoGo, negative correlation across participants, small volume correction (SPL; Fig. 4d)	1	R Superior Parietal Lobule	87	87	30	-40	44.5	3.92

Supplementary Table 3*. Passive viewing task, one month after minus before CAT: Regions with significant activation for the imaging contrasts of* ***Fig. 4****. For each cluster, the list presents all regions from the Harvard-Oxford atlas that contained at least 10 active voxels within the cluster, as well as the X/Y/Z location for the peak activation in MNI space.*

Contrast	Cluster	Region	Number of voxels in region	Cluster size	X	Y	Z	Peak z stat
Choices of high-value Go minus choices of high-value NoGo items (fig. 5a)	1	R Occipital Fusiform Gyrus	60	131	34	-60	-18	3.86
		R Temporal Occipital Fusiform Cortex	40					
		R Lingual Gyrus	29					
	2	L Central Opercular Cortex	59	136	-68	-12	12	3.74
		L Postcentral Gyrus	10					
	3	R Central Opercular Cortex	101	152	46	-10	7	3.91
		R Heschl's Gyrus (includes H1 and H2)	14					
		R Insular Cortex	13					
	4	L Middle Temporal Gyrus, temporooccipital part	65	188	-48	-60	12	4.04
		L Lateral Occipital Cortex, inferior division	44					
		L Angular Gyrus	24					
		L Lateral Occipital Cortex, superoir division	22					
		L Supramarginal Gyrus, posterior division	13					
Choices of high-value Go minus choices of high-value NoGo items, negative correlation across participants (Fig. 5b)	1	Right Thalamus	103	137	8	-26	2	3.91
	2	Left Caudate	70	148	-10	0	7	4
		Left Thalamus	17					
		Left Accumbens	16					
	3	R Frontal Operculum Cortex	93	187	30	28	4.5	4.17
		R Insular Cortex	22					
		R Frontal Orbital Cortex	20					

		R Inferior Frontal Gyrus, pars triangularis	12					
	4	L Frontal Operculum Cortex	76	269	-44	22	12	4.51
		L Frontal Orbital Cortex	52					
		L Inferior Frontal Gyrus, pars opercularis	31					
		L Insular Cortex	21					
	5	R Superior Frontal Gyrus	152	404	2	12	52	4.28
		L Juxtapositional Lobule Cortex (formerly Supplementary Motor Cortex)	77					
		R Juxtapositional Lobule Cortex (formerly Supplementary Motor Cortex)	60					
		R Paracingulate Gyrus	33					
		L Superior Frontal Gyrus	15					
Choices of high-value Go items, negative modulation across items (Fig. 5c)	1	R Superior Frontal Gyrus	99	143	26	8	60	3.98
		R Middle Frontal Gyrus	23					
	2	L Central Opercular Cortex	66	158	-48	-18	17	3.86
		L Parietal Operculum Cortex	62					
		L Planum Temporale	20					
	3	L Frontal Pole	93	225	-40	30	35	4.51
		L Middle Frontal Gyrus	86					
	4	R Paracingulate Gyrus	150	242	8	12	27	3.65

		R Cingulate Gyrus, anterior division	42					
		R Juxtapositional Lobule Cortex (formerly Supplementary Motor Cortex)	25					
	5	Right Putamen	58	245	32	16	2	3.88
		R Insular Cortex	47					
		Right Caudate	29					
		R Frontal Orbital Cortex	23					
		R Frontal Operculum Cortex	16					
	6	L Insular Cortex		280	-40	8	9.5	4.43
		L Frontal Operculum Cortex	57					
		L Central Opercular Cortex	47					
		Left Putamen	27					
		L Frontal Orbital Cortex	22					
	7	L Precentral Gyrus	172	365	-26	-6	67	4.15
		L Superior Frontal Gyrus	90					
		L Middle Frontal Gyrus	30					
Choices of high-value Go items, negative correlation across participants, small volume correction (SPL; Fig. 5d)	1	R Superior Parietal Lobule	53	53	34	-48	47	3.44

Choices of high-value Go items, negative modulation across items, small volume correction (SPL; Fig. 5e)	1	R Superior Parietal Lobule	47	47	26	-44	67	3.8

Supplementary Table 4. *Probe task, after CAT: Regions with significant activation for the imaging contrasts of* ***Fig. 5****. For each cluster, the list presents all regions from the Harvard-Oxford atlas that contained at least 10 active voxels within the cluster, as well as the X/Y/Z location for the peak activation in MNI space.*

Contrast	Cluster	Region	Number of voxels in region	Cluster size	X	Y	Z	Peak z stat
Choices of high-value Go items, modulation across items (Fig. 6a)	1	R Precuneous Cortex	117	151	6	-70	44.5	3.67
		L Precuneous Cortex	30					
	2	R Middle Temporal Gyrus, posterior division	92	175	54	-18	-3	3.89
		R Superior Temporal Gyrus, posterior division	62					
		R Superior Temporal Gyrus, anterior division	14					
	3	L Lateral Occipital Cortex, superoir division	108	201	-46	-64	24.5	4.18
		L Angular Gyrus	62					
	4	R Lateral Occipital Cortex, superoir division	205	208	52	-66	34.5	3.87
	5	L Middle Temporal Gyrus, posterior division	226	342	-56	-24	-10.5	4.3
		L Superior Temporal Gyrus, posterior division	69					
		L Middle Temporal Gyrus, temporooccipital part	23					
Choices of high-value Go items, correlation across participants (Fig. 6b)	1	R Postcentral Gyrus	68	181	64	-14	22	4.4
		R Parietal Operculum Cortex	42					
		R Planum Temporale	19					
		R Supramarginal Gyrus, anterior division	18					
	2	L Precuneous Cortex	134	474	2	-42	57	3.8
		R Precuneous Cortex	121					
		R Cingulate Gyrus, posterior division	111					
		L Cingulate Gyrus, posterior division	81					
		L Intracalcarine Cortex	10					

Supplementary Table 5. *Probe task, one month after CAT: Regions with significant activation for the imaging contrasts of* ***Fig. 6****. For each cluster, the list presents all*

regions from the Harvard-Oxford atlas that contained at least 10 active voxels within the cluster, as well as the X/Y/Z location for the peak activation in MNI space.